Science Advances
AAAS

advances.sciencemag.org/cgi/content/full/6/32/eabb5915/DC1

Supplementary Materials for

Nonadiabatic exciton-phonon coupling in Raman spectroscopy of layered materials

Sven Reichardt* and Ludger Wirtz

*Corresponding author. Email: sven.reichardt@uni.lu

Published 7 August 2020, *Sci. Adv.* **6**, eabb5915 (2020)
DOI: 10.1126/sciadv.abb5915

This PDF file includes:

S1. THEORETICAL DETAILS

Here we provide more details on how to obtain Eq. (3) from Eq. (2) of the main text.
We start from Eq. (2) of the main text,

$$\tilde{\mathcal{M}}^{\lambda}_{\mu\nu}(\omega',\omega) \equiv \frac{1}{\hbar^2}\int_{-\infty}^{+\infty} \mathrm{d}t\, \mathrm{e}^{i\omega t} \int_{-\infty}^{+\infty} \mathrm{d}t'\, \mathrm{e}^{i\omega' t'} (-i)\langle 0|\mathcal{T}\left[\hat{F}_\lambda(t')\hat{J}_\nu(t)\hat{J}^\dagger_\mu(0)\right]|0\rangle\big|_{\text{connect.}}, \tag{S1}$$

and first provide a definition of all the appearing quantities before proceeding with the derivation of Eq. (3) of the main text. The correlation function on the right-hand side involves: (i) the spatially Fourier-transformed electronic current density operator $\hat{J}$ in the dipole approximation, projected onto the light polarization vector $\boldsymbol{\epsilon}_\mu$:

$$\hat{J}_\mu \equiv (-e/m)\boldsymbol{\epsilon}^*_\mu \cdot \int \mathrm{d}^3 r\, \hat{\psi}^\dagger(\mathbf{r})(-i\hbar\boldsymbol{\nabla})\hat{\psi}(\mathbf{r}) \tag{S2}$$

and (ii) the electronic force operator $\hat{F}_\lambda$, projected onto the eigenvector of a zero-momentum phonon mode λ:

$$\hat{F}_\lambda \equiv \sum_I \mathbf{v}^\lambda_I \cdot \int \mathrm{d}^3 r\, \hat{\psi}^\dagger(\mathbf{r})\hat{\psi}(\mathbf{r})\partial V_{\text{lat}}(\mathbf{r})/\partial(\mathbf{R}_I)|_{\{\mathbf{R}^{(0)}_I\}}. \tag{S3}$$

In the latter, the sum over I runs over all atoms and $\mathbf{v}^\lambda_I$ denotes the displacement vector (with dimensions of length) of atom I according to the zero-momentum phonon mode λ. Further, $V_{\text{lat}}(\mathbf{r})$ denotes a fixed lattice potential of nuclei with equilibrium configuration $\{\mathbf{R}^{(0)}_I\}$ and $\hat{\psi}(\mathbf{r})$ is the electron field operator, with $(-e)$ and m being the charge and mass of an electron, respectively. Finally, all time-dependent operators are understood to be in the Heisenberg picture with respect to the full Hamiltonian of the matter system, whose ground state is denoted by $|0\rangle$.

The challenge in making the scattering matrix element of Eq. (S1) accessible to a numerical computation lies in the complexity of the three-particle correlation function appearing as part of the force-current-current correlation function. In order to find an approximation for it that still captures excitonic and non-adiabatic effects, we treat both the electron-electron and the electron-phonon interaction in perturbation theory and carry out a diagrammatic analysis. This allows us to systematically truncate the perturbation series in a way that captures the relevant physics, but can still be evaluated in a way suitable for a numerical calculation.

To start with, we expand the bare (b) electronic current density and force operators in the basis of Kohn-Sham states:

$$\hat{J}_\mu \equiv \sum_{\mathbf{k},a,a'} \left(d^{\mu,(\mathrm{b})}_{\mathbf{k},a',a}\right)^* \hat{c}^\dagger_{\mathbf{k},a}\hat{c}_{\mathbf{k},a'} \tag{S4}$$

$$\hat{F}_\lambda \equiv \sum_{\mathbf{k},b,b'} \left(g^{\lambda,(\mathrm{b})}_{\mathbf{k},b',b}\right)^* \hat{c}^\dagger_{\mathbf{k},b}\hat{c}_{\mathbf{k},b'}. \tag{S5}$$

The expansion coefficients are defined such that they denote the matrix elements for *photon/phonon emission*, i.e., *current density/force annihilation*. Note that at zero momentum transfer and for real polarization vectors/phonon eigenvectors, the matrix elements obey $m^{(\mathrm{b})}_{\mathbf{k},a',a} = \left(m^{(\mathrm{b})}_{\mathbf{k},a,a'}\right)^*$.

In terms of these matrix elements, the time-ordered force-current-current correlation function reads

$$\begin{aligned}\langle 0|\mathcal{T}\left[\hat{F}_\lambda(t')\hat{J}_\nu(t)\hat{J}^\dagger_\mu(0)\right]|0\rangle\big|_{\text{connect.}} = &\sum_{\mathbf{k},\mathbf{k}',\mathbf{k}''}\sum_{\substack{a,b,c\\a',b',c'}} \left(g^{\lambda,(\mathrm{b})}_{\mathbf{k},a',a}\right)^* \left(d^{\nu,(\mathrm{b})}_{\mathbf{k}',b',b}\right)^* d^{\mu,(\mathrm{b})}_{\mathbf{k}'',c,c'} \\ &\times \langle 0|\mathcal{T}\left[\hat{c}^\dagger_{\mathbf{k},a}(t')\hat{c}_{\mathbf{k},a'}(t')\hat{c}^\dagger_{\mathbf{k}',b}(t)\hat{c}_{\mathbf{k}',b'}(t)\hat{c}^\dagger_{\mathbf{k}'',c}(0)\hat{c}_{\mathbf{k}'',c'}(0)\right]|0\rangle\big|_{\text{connect.}}.\end{aligned} \tag{S6}$$

The last factor is the fully connected part of the three-particle Green's function. We approximate it in a controlled way with the help of Feynman diagrams, as shown in Fig. S1. The first term shown corresponds to the independent-particle

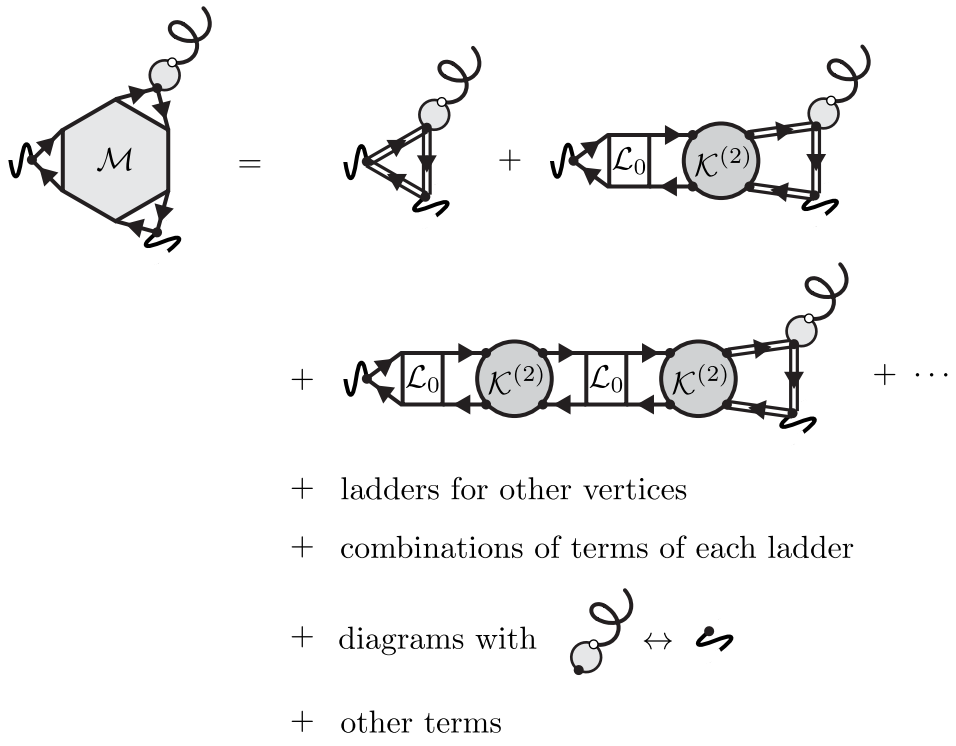

FIG. S1. **Diagrammatic analysis of the scattering matrix element.** Dark dots (light circles) denote the bare electron-photon (-phonon) vertex. Double lines denote the one-electron Green's function. $\mathcal{L}$ ($\mathcal{L}_0$) and $\mathcal{K}^{(2)}$ denote the interacting (independent-particle) two-particle correlation function and two-particle interaction kernel, respectively.

approximation to the three-particle correlation function. In the second term, we include the first-order correction to the electron-incoming photon vertex due to two-particle inter-electron interactions. We denote the kernel describing the latter by $\mathcal{K}^{(2)}$, while $\mathcal{L}_0$ represents the two-particle correlation function on the independent-particle level. The second line shows the second-order correction to the same vertex while the dots refer to higher-order corrections of the same form. We consider the same summation of terms for all three vertices simultaneously. In order to consider all topologically distinct diagrams, we also need to consider terms in which the fermion flow is reversed, i.e., in which the vertices for the outgoing photon and phonon are interchanged.

We do now adopt what we refer to as the *ladder-like approximation* in the following. It consists of neglecting all terms that do not follow the ladder-like structure depicted in the first two lines of Fig. S1. As shown in Fig. S2, the summation of terms at each vertex can be carried out separately. The double Fourier transform of the force-current-current correlation function, which up to a factor of i corresponds to the scattering matrix element, then takes on the form

$$\begin{aligned} i\tilde{\mathcal{M}}^{\lambda}_{\mu\nu}(\omega',\omega) = &\sum_{\mathbf{k}} \sum_{\substack{a,b,c \\ a',b',c'}} \overline{g}^{\lambda}_{\mathbf{k},a',a}(\omega')\overline{d}^{\nu}_{\mathbf{k},b',b}(\omega) d^{\mu}_{\mathbf{k},c,c'}(\omega+\omega') \\ &\times \frac{1}{\hbar^2}\int_{-\infty}^{+\infty} \mathrm{d}t\, \mathrm{e}^{i\omega t} \int_{-\infty}^{+\infty} \mathrm{d}t'\, \mathrm{e}^{i\omega' t'} \langle 0|\mathcal{T}\left[\hat{c}^{\dagger}_{\mathbf{k},a}(t')\hat{c}_{\mathbf{k},a'}(t')\hat{c}^{\dagger}_{\mathbf{k},b}(t)\hat{c}_{\mathbf{k},b'}(t)\hat{c}^{\dagger}_{\mathbf{k},c}(0)\hat{c}_{\mathbf{k},c'}(0)\right]|0\rangle\big|_{\mathrm{IP,connect.}}, \end{aligned} \tag{S7}$$

where the three-particle correlation function now only appears in the form of its independent-particle version. The first three factors denote the Fourier transforms of the *exact* vertices, with a bar denoting the vertices for photon/phonon emission. To obtain concrete expressions for the latter, we approximate the two-particle interaction kernel as described in the following.

In the case of the electron-light vertex, we approximate it as the sum of a statically screened, attractive electron-hole Coulomb interaction and a bare, repulsive exchange part. We can then give an explicit expression for the

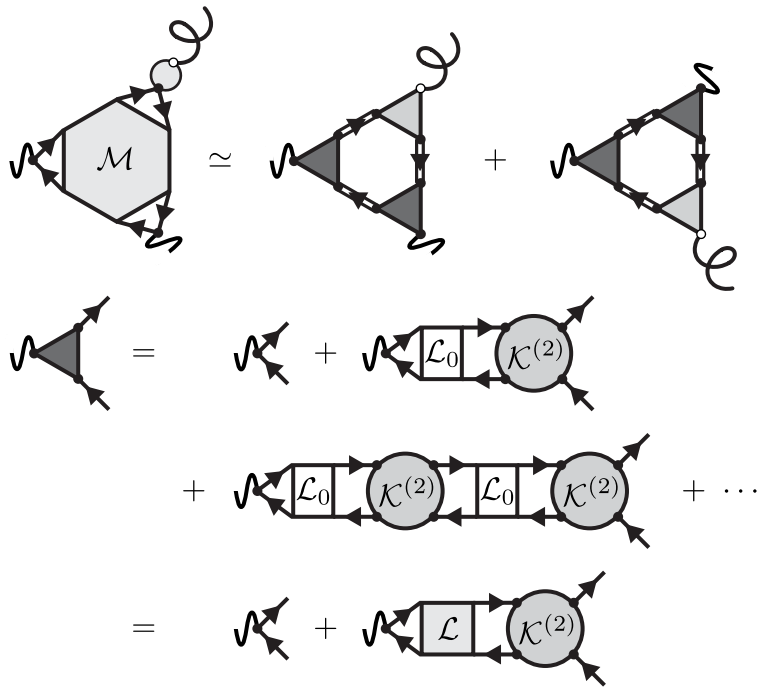

FIG. S2. **Ladder-like approximation to the scattering matrix element.** Top: Diagrammatic approximation for the scattering matrix element (left) as a sum of two terms with effectively opposite orientation of the fermion loop. Dark dots (light circles) denote the bare electron-photon (-phonon) vertex. Double lines denote the one-electron Green's function. Dark (light) shaded triangles the exact electron-photon (-phonon) vertex. Bottom: Exact ladder of diagrams for the electron-light coupling. $\mathcal{L}$ ($\mathcal{L}_0$) and $\mathcal{K}^{(2)}$ denote the interacting (independent-particle) two-particle correlation function and two-particle interaction kernel, respectively. Note that the same summation is understood to be carried out at each vertex.

Fourier-transformed vertex function by making use of the Bethe-Salpeter equation

$$L_{\substack{\mathbf{k},a',a\\ \mathbf{k}',b',b}}(\omega) = L_{0;\mathbf{k},a',a}(\omega)\delta_{\mathbf{k},\mathbf{k}'}\delta_{a',b'}\delta_{a,b} + L_{0;\mathbf{k},a',a}(\omega)\sum_{\mathbf{k}''}\sum_{c',c} K^{(2)}_{\substack{\mathbf{k},a',a\\ \mathbf{k}'',c',c}} L_{\substack{\mathbf{k}'',c',c\\ \mathbf{k}',b',b}}(\omega) \tag{S8}$$

where we now use non-calligraphic script to denote the approximated quantities. Note that we also use the quasi-particle approximation for L_0, so that it only depends on two band indices. As shown in Fig. S2, we can identify the right-hand side up to a factor of L_0 as the factor that modulates the bare vertex, and we thus have

$$d^{\mu}_{\mathbf{k},a',a}(\omega) = d^{\mu,(\mathrm{b})}_{\mathbf{k},a',a} + \sum_{\mathbf{k}',\mathbf{k}''}\sum_{\substack{b',c'\\ b,c}} K^{(2)}_{\substack{\mathbf{k},a',a\\ \mathbf{k}',b',b}} L_{\substack{\mathbf{k}',b',b\\ \mathbf{k}'',c',c}}(\omega) d^{\mu,(\mathrm{b})}_{\mathbf{k}'',c',c} = L^{-1}_{0;\mathbf{k},a',a}(\omega)\sum_{\mathbf{k}'}\sum_{b',b} L_{\substack{\mathbf{k},a',a\\ \mathbf{k}',b',b}}(\omega) d^{\mu,(\mathrm{b})}_{\mathbf{k}',b',b} \tag{S9}$$

for photon *absorption* and

$$\overline{d}^{\mu}_{\mathbf{k},a',a}(\omega) = \left(d^{\mu,(\mathrm{b})}_{\mathbf{k},a',a}\right)^* + \sum_{\mathbf{k}',\mathbf{k}''}\sum_{\substack{b',c'\\ b,c}} \left(d^{\mu,(\mathrm{b})}_{\mathbf{k}',b',b}\right)^* L_{\substack{\mathbf{k}',b',b\\ \mathbf{k}'',c',c}}(\omega) K^{(2)}_{\substack{\mathbf{k}'',c',c\\ \mathbf{k},a',a}} = \sum_{\mathbf{k}'}\sum_{b',b} \left(d^{\mu,(\mathrm{b})}_{\mathbf{k}',b',b}\right)^* L_{\substack{\mathbf{k}',b',b\\ \mathbf{k},a',a}}(\omega) L^{-1}_{0;\mathbf{k},a',a}(\omega). \tag{S10}$$

for photon *emission*. Lastly, as mentioned in the main text, we also use the *Tamm-Dancoff approximation*, which is justified for the semiconducting systems discussed in the main text. In this approximation, the independent-particle two-particle correlation function reads

$$L_{0;\mathbf{k},a',a}(\omega) = \frac{\bar{f}_{\mathbf{k},a'} f_{\mathbf{k},a}}{\hbar\omega - (\varepsilon_{\mathbf{k},a'} - \varepsilon_{\mathbf{k},a}) + i\eta} + \frac{f_{\mathbf{k},a'} \bar{f}_{\mathbf{k},a}}{-\hbar\omega - (\varepsilon_{\mathbf{k},a} - \varepsilon_{\mathbf{k},a'}) + i\eta}, \tag{S11}$$

where $f_{\mathbf{k},a}$ denotes the occupancy of the state $|\mathbf{k},a\rangle$ in the ground state, $\bar{f}_{\mathbf{k},a} \equiv 1 - f_{\mathbf{k},a}$, and η is a positive infinitesimal. The interacting two-particle correlation function can be expressed in terms of the excitonic wave functions $A^S_{\mathbf{k},a',a}$ and energies E_S as

$$L_{\substack{\mathbf{k},a',a \\ \mathbf{k}',b',b}}(\omega) = \sum_S \left[\bar{f}_{\mathbf{k},a'} f_{\mathbf{k},a} \bar{f}_{\mathbf{k}',b'} f_{\mathbf{k}',b} \frac{A^S_{\mathbf{k},a',a} \left(A^S_{\mathbf{k}',b',b}\right)^*}{\hbar\omega - E_S + i\eta} + f_{\mathbf{k},a'} \bar{f}_{\mathbf{k},a} f_{\mathbf{k}',b'} \bar{f}_{\mathbf{k}',b} \frac{\left(A^S_{\mathbf{k},a,a'}\right)^* A^S_{\mathbf{k}',b,b'}}{-\hbar\omega - E_S + i\eta} \right], \tag{S12}$$

where the sum runs over all *positive-energy* excitons. Note that within the Tamm-Dancoff approximation, an excitonic envelope wave function $A^S_{\mathbf{k},a',a}$ for positive-energy excitons has non-vanishing components only for $a' \in \mathcal{C}$ and $a \in \mathcal{V}$, where $\mathcal{C}$ and $\mathcal{V}$ denote the sets of conduction and valence band indices, respectively. Combining the last three equations, we arrive at the final expression we use to approximate the exact electron-photon vertices:

$$\begin{aligned} d^\mu_{\mathbf{k},a',a}(\omega) = \sum_S \Bigg[& \bar{f}_{\mathbf{k},a'} f_{\mathbf{k},a} A^S_{\mathbf{k},a',a} \frac{\hbar\omega - (\varepsilon_{\mathbf{k},a'} - \varepsilon_{\mathbf{k},a}) + i\eta}{\hbar\omega - E_S + i\eta} d^\mu_S \\ & + f_{\mathbf{k},a'} \bar{f}_{\mathbf{k},a} \left(A^S_{\mathbf{k},a,a'}\right)^* \frac{-\hbar\omega - (\varepsilon_{\mathbf{k},a} - \varepsilon_{\mathbf{k},a'}) + i\eta}{-\hbar\omega - E_S + i\eta} \left(d^\mu_S\right)^* \Bigg] \end{aligned} \tag{S13}$$

and

$$\begin{aligned} \bar{d}^\mu_{\mathbf{k},a',a}(\omega) = \sum_S \Bigg[& \bar{f}_{\mathbf{k},a'} f_{\mathbf{k},a} \left(d^\mu_S\right)^* \frac{\hbar\omega - (\varepsilon_{\mathbf{k},a'} - \varepsilon_{\mathbf{k},a}) + i\eta}{\hbar\omega - E_S + i\eta} \left(A^S_{\mathbf{k},a',a}\right)^* \\ & + f_{\mathbf{k},a'} \bar{f}_{\mathbf{k},a} d^\mu_S \frac{-\hbar\omega - (\varepsilon_{\mathbf{k},a} - \varepsilon_{\mathbf{k},a'}) + i\eta}{-\hbar\omega - E_S + i\eta} A^S_{\mathbf{k},a,a'} \Bigg], \end{aligned} \tag{S14}$$

with d^μ_S as defined in Eq. (4) of the main text.

For the exact electron-phonon vertex, we follow the same line of argument, but approximate the two-particle interaction kernel in that case with the kernel corresponding to time-dependent density functional theory. As shown in Secs. 4.3 and 4.5 of Ref. (29), this approximation is exactly equivalent to using the statically screened electron-phonon coupling on the level of density functional perturbation theory. In addition, we also neglect the frequency dependence of the vertex function, i.e., we use

$$\bar{g}^\lambda_{\mathbf{k},a',a}(\omega) \to \left(g^\lambda_{\mathbf{k},a',a}\right)^* \big|_{\mathrm{DFPT}}, \tag{S15}$$

which is justified for systems with a band gap much larger than the phonon frequency. Note, however, that we *do retain the phonon frequency-dependence of the three-particle independent-particle correlation function* as there the frequency of the photon needs to be considered as well, which reduces the effective band gap seen by the phonon in the three-particle correlation function.

Finally, we also give the explicit form of the Fourier transformed independent-particle three-particle correlation function. Treating it on the level of the quasi-particle approximation, one finds

$$\begin{aligned} & \frac{1}{\hbar^2} \int_{-\infty}^{+\infty} \mathrm{d}t\, \mathrm{e}^{i\omega t} \int_{-\infty}^{+\infty} \mathrm{d}t'\, \mathrm{e}^{i\omega' t'} \langle 0 | \mathcal{T} \left[\hat{c}^\dagger_{\mathbf{k},a}(t') \hat{c}_{\mathbf{k},a'}(t') \hat{c}^\dagger_{\mathbf{k},b}(t) \hat{c}_{\mathbf{k},b'}(t) \hat{c}^\dagger_{\mathbf{k},c}(0) \hat{c}_{\mathbf{k},c'}(0) \right] |0\rangle \big|_{\mathrm{IP,connect.}} \\ = & \frac{1}{\hbar^2} \int_{-\infty}^{+\infty} \mathrm{d}t\, \mathrm{e}^{i\omega t} \int_{-\infty}^{+\infty} \mathrm{d}t'\, \mathrm{e}^{i\omega' t'} (-1) \\ & \times \Big\{ \delta_{a',b} \delta_{b',c} \delta_{c',a} \langle 0 | \mathcal{T} \left[\hat{c}_{\mathbf{k},a}(t') \hat{c}^\dagger_{\mathbf{k},a}(t) \right] |0\rangle \langle 0 | \mathcal{T} \left[\hat{c}_{\mathbf{k},b}(t) \hat{c}^\dagger_{\mathbf{k},b}(0) \right] |0\rangle \langle 0 | \mathcal{T} \left[\hat{c}_{\mathbf{k},c}(0) \hat{c}^\dagger_{\mathbf{k},c}(t') \right] |0\rangle \\ & \quad + \delta_{a',c} \delta_{c',b} \delta_{b',a} \langle 0 | \mathcal{T} \left[\hat{c}_{\mathbf{k},a}(t') \hat{c}^\dagger_{\mathbf{k},a}(0) \right] |0\rangle \langle 0 | \mathcal{T} \left[\hat{c}_{\mathbf{k},b}(t) \hat{c}^\dagger_{\mathbf{k},b}(t') \right] |0\rangle \langle 0 | \mathcal{T} \left[\hat{c}_{\mathbf{k},c}(0) \hat{c}^\dagger_{\mathbf{k},c}(t) \right] |0\rangle \Big\} \\ \equiv & \, i\, \delta_{a',b} \delta_{b',c} \delta_{c',a} R_{0;\mathbf{k},c,a,b}(-\omega', -\omega) + i\, \delta_{a',c} \delta_{c',b} \delta_{b',a} R_{0;\mathbf{k},a,b,c}(\omega', \omega). \end{aligned} \tag{S16}$$

In the last step, we identified the Fourier transform of the independent-particle three-particle correlation function on

the quasi-particle level, which is explicitly given by

$$
\begin{aligned}
&(-i)R_{0;\mathbf{k},a,b,c}(\omega_1,\omega_2)\\
=&\frac{1}{\hbar^2}\int_{-\infty}^{+\infty}\mathrm{d}t\,\mathrm{e}^{i\omega t}\int_{-\infty}^{+\infty}\mathrm{d}t'\,\mathrm{e}^{i\omega' t'}\langle 0|\mathcal{T}\left[\hat{c}_{\mathbf{k},a}(t')\hat{c}^{\dagger}_{\mathbf{k},a}(0)\right]|0\rangle\langle 0|\mathcal{T}\left[\hat{c}_{\mathbf{k},b}(t)\hat{c}^{\dagger}_{\mathbf{k},b}(t')\right]|0\rangle\langle 0|\mathcal{T}\left[\hat{c}_{\mathbf{k},c}(0)\hat{c}^{\dagger}_{\mathbf{k},c}(t)\right]|0\rangle\\
=&+\frac{f_{\mathbf{k},a}\bar{f}_{\mathbf{k},b}\bar{f}_{\mathbf{k},c}}{[-\hbar\omega_1-\hbar\omega_2-(\varepsilon_{\mathbf{k},c}-\varepsilon_{\mathbf{k},a})+i\eta][-\hbar\omega_1-(\varepsilon_{\mathbf{k},b}-\varepsilon_{\mathbf{k},a})+i\eta]}\\
&-\frac{\bar{f}_{\mathbf{k},a}f_{\mathbf{k},b}f_{\mathbf{k},c}}{[\hbar\omega_1+\hbar\omega_2-(\varepsilon_{\mathbf{k},a}-\varepsilon_{\mathbf{k},c})+i\eta][\hbar\omega_1-(\varepsilon_{\mathbf{k},a}-\varepsilon_{\mathbf{k},b})+i\eta]}\\
&+\frac{\bar{f}_{\mathbf{k},a}\bar{f}_{\mathbf{k},b}f_{\mathbf{k},c}}{[\hbar\omega_1+\hbar\omega_2-(\varepsilon_{\mathbf{k},a}-\varepsilon_{\mathbf{k},c})+i\eta][\hbar\omega_2-(\varepsilon_{\mathbf{k},b}-\varepsilon_{\mathbf{k},c})+i\eta]}\\
&-\frac{f_{\mathbf{k},a}f_{\mathbf{k},b}\bar{f}_{\mathbf{k},c}}{[-\hbar\omega_1-\hbar\omega_2-(\varepsilon_{\mathbf{k},c}-\varepsilon_{\mathbf{k},a})+i\eta][-\hbar\omega_2-(\varepsilon_{\mathbf{k},c}-\varepsilon_{\mathbf{k},b})+i\eta]}\\
&+\frac{\bar{f}_{\mathbf{k},a}f_{\mathbf{k},b}\bar{f}_{\mathbf{k},c}}{[\hbar\omega_1-(\varepsilon_{\mathbf{k},a}-\varepsilon_{\mathbf{k},b})+i\eta][-\hbar\omega_2-(\varepsilon_{\mathbf{k},c}-\varepsilon_{\mathbf{k},b})+i\eta]}\\
&-\frac{f_{\mathbf{k},a}\bar{f}_{\mathbf{k},b}f_{\mathbf{k},c}}{[-\hbar\omega_1-(\varepsilon_{\mathbf{k},b}-\varepsilon_{\mathbf{k},a})+i\eta][\hbar\omega_2-(\varepsilon_{\mathbf{k},b}-\varepsilon_{\mathbf{k},c})+i\eta]}.
\end{aligned}
\tag{S17}
$$

It is then straightforward to obtain Eqs. (3-5) from the main text by combining all of the individual pieces and replacing η by the electronic broadening γ.

S2. COMPUTATIONAL DETAILS FOR THE HBN AND MOS_2 CALCULATIONS

Here we present material-specific information regarding the first-principles calculations.

hBN

The ground state properties of bulk hexagonal boron nitride in the AA' stacking configuration were obtained using norm-conserving, non-relativistic, core-corrected pseudopotentials. We use a plane-wave basis set with an energy cutoff of 110 Ry for the electronic wave functions and 440 Ry for the charge density. For integrations over the first Brillouin zone, a uniform **k**-point mesh of size 12×12×2 was used. The lattice parameters were relaxed prior to the calculation, yielding values of a=2.478 Å and c=6.453 Å for the in- and out-of-plane lattice constants, respectively. For the electronic excited state properties, we computed the electronic band structure on a 36×36×2 **k**-point mesh for 200 (spin-degenerate) bands. We included the upper two valence and lower two conduction bands in the construction of the two-particle interaction kernel. A rigid band energy shift of 2 eV was added to all independent-particle transition energies in order to account for the underestimation of the band gap in DFT. This value was obtained in previous first-principles calculations on the level of the GW approximation (20). Lastly, for the phonon frequency of the degenerate, Raman-active in-plane optical mode (E_{2g}-symmetry), we use the calculated value of 1388.6 cm^{-1}.

MoS_2

The ground state properties of monolayer molybdenum disulfide were computed using norm-conserving, fully relativistic pseudopotentials for both sulfur and molybdenum to account for the effects of spin-orbit interactions. We use a plane-wave basis set with an energy cutoff of 90 Ry for the electronic wave functions and 360 Ry for the charge density. For integrations over the first Brillouin zone, a uniform **k**-point mesh of size 12×12×1 was used. The lattice parameter was relaxed prior to the calculation, yielding a value of a=3.170 Å for the in-plane lattice constant. To preserve the single-layer nature of the system, we use a vacuum spacing of 16 Å between periodic images of the monolayer. For the electronic excited state properties, we computed the electronic band structure on a 24×24×1 **k**-point mesh with spin-orbit coupling for 400 (in general spin-non-degenerate) bands. We included the upper eight valence and lower eight conduction bands in the construction of the two-particle interaction kernel. A rigid band energy shift of 0.925 eV was added to all independent-particle transition energies in order to account for the underestimation of the band gap in DFT. This value was obtained in previous first-principles calculations on the level of the GW approximation (21). Lastly, for the phonon frequencies of the degenerate, Raman-active in-plane optical mode of E'-symmetry and the non-degenerate out-of-plane mode of A_1'-symmetry, we use the previously calculated values of 391.7 cm^{-1} and 410.3 cm^{-1} (36).